Long-time existence of Brownian motion on configurations of two landmarks

Talk by Karen Habermann *on joint work with*
Philipp Harms and Stefan Sommer

Bulletin of the London Mathematical Society, Vol. 56 (2024), No. 5, 1658–1679

Geometric Sciences in Action: from geometric statistics to shape analysis (CIRM, Luminy, May 2024)

Motivation: Phylogenetic trees

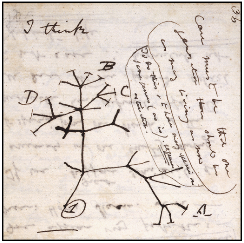

© Darwin

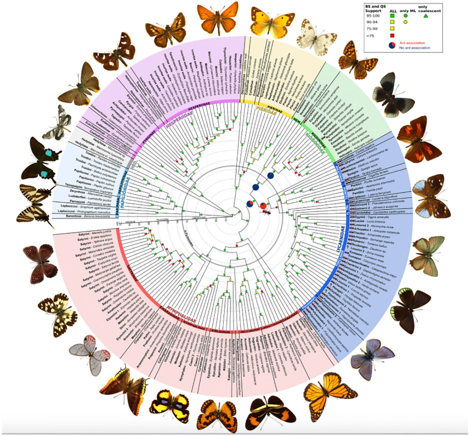

© Espeland et al.

Motivation: Matching MRI scans

- Templates can be used for the identification of structures in Magnetic Resonance Images (MRI) of brains.
  - Template can represent the prototypical structure of the brain of someone developing Alzheimer's disease.
  - Templates are matched to the MRI scan of an individual.
- Interpolating time dependent data which may arise as a result of follow-up studies of the brain or which are given in the form of historical data such as butterfly wing shapes.

Motivation: Matching MRI scans

- Templates can be used for the identification of structures in Magnetic Resonance Images (MRI) of brains.
  - Template can represent the prototypical structure of the brain of someone developing Alzheimer's disease.
  - Templates are matched to the MRI scan of an individual.
- Interpolating time dependent data which may arise as a result of follow-up studies of the brain or which are given in the form of historical data such as butterfly wing shapes.

- **Imagery are assumed characterised via sets of landmarks:** To reduce the analysis to objects in a finite dimensional space, the boundary of a shape in $\mathbb{R}^d$ for $d \geq 2$ is commonly represented by a sequence of n distinct points in $\mathbb{R}^d$.

Landmark configuration spaces

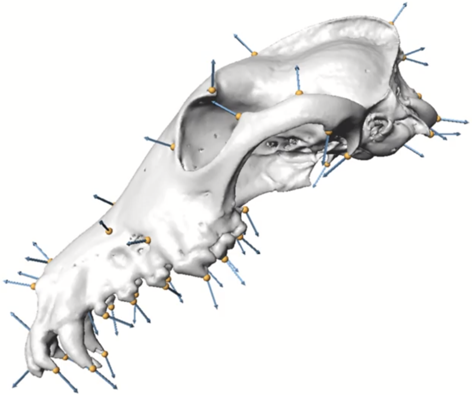

© Hipsley

Large Deformation Diffeomorphisms Landmark Matching

Large Deformation Diffeomorphisms Landmark Matching

- Large Deformation Diffeomorphic Metric Mapping (LDDMM) framework models shape variations as diffeomorphic deformations.

Large Deformation Diffeomorphisms Landmark Matching

- Large Deformation Diffeomorphic Metric Mapping (LDDMM) framework models shape variations as diffeomorphic deformations.
- The optimal diffeomorphic match is constructed to minimise a running smoothness cost $\|Lv\|^2$ associated with a differential operator L on the velocity field generating diffeomorphisms whilst simultaneously minimising the matching end point condition of the landmarks.

Large Deformation Diffeomorphisms Landmark Matching

- Large Deformation Diffeomorphic Metric Mapping (LDDMM) framework models shape variations as diffeomorphic deformations.
- The optimal diffeomorphic match is constructed to minimise a running smoothness cost $\|Lv\|^2$ associated with a differential operator L on the velocity field generating diffeomorphisms whilst simultaneously minimising the matching end point condition of the landmarks.
- In diffeomorphic landmark matching two landmark configurations $q, p \in Q$ are matched by solving the optimisation problem

$$\min_u \int_0^1 \|u_t\|_V^2 \, \mathrm{d}t \quad \text{subject to} \quad \varphi_1.q = p$$

where $\frac{\partial \varphi_t}{\partial t} = u_t \circ \varphi_t$ with $\varphi_0 = \mathrm{Id}_{\mathbb{R}^d}$.

Large Deformation Diffeomorphisms Landmark Matching

- Two landmark configurations $q, p \in Q$ are matched by solving the optimisation problem

$$\min_u \int_0^1 \|u_t\|_V^2 \,\mathrm{d}t \quad \text{subject to} \quad \varphi_1.q = p$$

where $\frac{\partial \varphi_t}{\partial t} = u_t \circ \varphi_t$ with $\varphi_0 = \mathrm{Id}_{\mathbb{R}^d}$.

Large Deformation Diffeomorphisms Landmark Matching

- Two landmark configurations $q, p \in Q$ are matched by solving the optimisation problem

$$\min_u \int_0^1 \|u_t\|_V^2 \, \mathrm{d}t \quad \text{subject to} \quad \varphi_1.q = p$$

  where $\frac{\partial \varphi_t}{\partial t} = u_t \circ \varphi_t$ with $\varphi_0 = \mathrm{Id}_{\mathbb{R}^d}$.
- Norm $\|\cdot\|_V$ stems from an inner product $\langle \cdot, \cdot \rangle_V$ on $\mathfrak{X}_c(\mathbb{R}^d)$ such that the completion of $\mathfrak{X}_c(\mathbb{R}^d)$ with respect to this norm is a Hilbert space V with positive reproducing kernel $K \colon \mathbb{R}^d \times \mathbb{R}^d \to \mathbb{R}^{d \times d}$.

Large Deformation Diffeomorphisms Landmark Matching

- Two landmark configurations $q, p \in Q$ are matched by solving the optimisation problem

$$\min_u \int_0^1 \|u_t\|_V^2 \,\mathrm{d}t \quad \text{subject to} \quad \varphi_1.q = p$$

  where $\frac{\partial \varphi_t}{\partial t} = u_t \circ \varphi_t$ with $\varphi_0 = \mathrm{Id}_{\mathbb{R}^d}$.
- Norm $\|\cdot\|_V$ stems from an inner product $\langle \cdot, \cdot \rangle_V$ on $\mathfrak{X}_c(\mathbb{R}^d)$ such that the completion of $\mathfrak{X}_c(\mathbb{R}^d)$ with respect to this norm is a Hilbert space V with positive reproducing kernel $K\colon \mathbb{R}^d \times \mathbb{R}^d \to \mathbb{R}^{d\times d}$.
- The optimisation problem is equivalent to the geodesic boundary value problem for a suitable Riemannian metric g on Q, and any minimiser u generates a diffeomorphic flow $\varphi\colon [0,1] \to \mathrm{Diff}_c(\mathbb{R}^d)$ which projects down to a geodesic in Q.

Large Deformation Diffeomorphisms Landmark Matching

- Norm $\|\cdot\|_V$ stems from an inner product $\langle\cdot,\cdot\rangle_V$ on $\mathfrak{X}_c(\mathbb{R}^d)$ such that the completion of $\mathfrak{X}_c(\mathbb{R}^d)$ with respect to this norm is a Hilbert space V with positive reproducing kernel $K\colon \mathbb{R}^d \times \mathbb{R}^d \to \mathbb{R}^{d\times d}$.
- The optimisation problem is equivalent to the geodesic boundary value problem for a suitable Riemannian metric g on Q, and any minimiser u generates a diffeomorphic flow $\varphi\colon [0,1] \to \mathrm{Diff}_c(\mathbb{R}^d)$ which projects down to a geodesic in Q.

Large Deformation Diffeomorphisms Landmark Matching

- Norm $\|\cdot\|_V$ stems from an inner product $\langle\cdot,\cdot\rangle_V$ on $\mathfrak{X}_c(\mathbb{R}^d)$ such that the completion of $\mathfrak{X}_c(\mathbb{R}^d)$ with respect to this norm is a Hilbert space V with positive reproducing kernel $K\colon \mathbb{R}^d \times \mathbb{R}^d \to \mathbb{R}^{d\times d}$.
- The optimisation problem is equivalent to the geodesic boundary value problem for a suitable Riemannian metric g on Q, and any minimiser u generates a diffeomorphic flow $\varphi\colon [0,1] \to \mathrm{Diff}_c(\mathbb{R}^d)$ which projects down to a geodesic in Q.
- The cometric g^{-1} admits a simple description in terms of the reproducing kernel K, namely, for $q \in Q$ and covectors $\xi, \eta \in T_q^* Q$,

$$g_q^{-1}(\xi,\eta) = \sum_{i,j=1}^{n} \xi_i^\top K(q_i,q_j)\eta_j \ .$$

Large Deformation Diffeomorphisms Landmark Matching

- Norm $\|\cdot\|_V$ stems from an inner product $\langle\cdot,\cdot\rangle_V$ on $\mathfrak{X}_c(\mathbb{R}^d)$ such that the completion of $\mathfrak{X}_c(\mathbb{R}^d)$ with respect to this norm is a Hilbert space V with positive reproducing kernel $K\colon \mathbb{R}^d \times \mathbb{R}^d \to \mathbb{R}^{d\times d}$.
- The optimisation problem is equivalent to the geodesic boundary value problem for a suitable Riemannian metric g on Q, and any minimiser u generates a diffeomorphic flow $\varphi\colon [0,1] \to \mathrm{Diff}_c(\mathbb{R}^d)$ which projects down to a geodesic in Q.
- The cometric g^{-1} admits a simple description in terms of the reproducing kernel K, namely, for $q \in Q$ and covectors $\xi, \eta \in T_q^* Q$,

$$g_q^{-1}(\xi,\eta) = \sum_{i,j=1}^{n} \xi_i^\top K(q_i,q_j)\eta_j \ .$$

Our analysis is based on this formula alone and does not make use of its geometric origins.

Large Deformation Diffeomorphisms Landmark Matching

- The cometric g^{-1} admits a simple description in terms of the reproducing kernel K, namely, for $q \in Q$ and covectors $\xi, \eta \in T_q^* Q$,

$$g_q^{-1}(\xi, \eta) = \sum_{i,j=1}^{n} \xi_i^\top K(q_i, q_j) \eta_j \ .$$

Large Deformation Diffeomorphisms Landmark Matching

- The cometric g^{-1} admits a simple description in terms of the reproducing kernel K, namely, for $q \in Q$ and covectors $\xi, \eta \in T_q^*Q$,

$$g_q^{-1}(\xi, \eta) = \sum_{i,j=1}^{n} \xi_i^\top K(q_i, q_j)\eta_j \ .$$

- We restrict our attention to kernels which are invariant under rotations and translations. This assumption is satisfied in most important examples.

Large Deformation Diffeomorphisms Landmark Matching

- The cometric g^{-1} admits a simple description in terms of the reproducing kernel K, namely, for $q \in Q$ and covectors $\xi, \eta \in T_q^* Q$,

$$g_q^{-1}(\xi, \eta) = \sum_{i,j=1}^{n} \xi_i^\top K(q_i, q_j) \eta_j \ .$$

- We restrict our attention to kernels which are invariant under rotations and translations. This assumption is satisfied in most important examples.
- We consider positive definite kernels of the form

$$K \colon \mathbb{R}^d \times \mathbb{R}^d \to \mathbb{R}^{d \times d}, \qquad (q_i, q_j) \mapsto k(\|q_i - q_j\|_{\mathbb{R}^d}) I_d$$

where $k \colon (0, \infty) \to \mathbb{R}$ is a scalar function.

Large Deformation Diffeomorphisms Landmark Matching

- We restrict our attention to kernels which are invariant under rotations and translations. This assumption is satisfied in most important examples.
- We consider positive definite kernels of the form

$$K\colon \mathbb{R}^d \times \mathbb{R}^d \to \mathbb{R}^{d\times d}, \qquad (q_i, q_j) \mapsto k(\|q_i - q_j\|_{\mathbb{R}^d}) I_d$$

where $k\colon (0,\infty) \to \mathbb{R}$ is a scalar function.

Large Deformation Diffeomorphisms Landmark Matching

- We restrict our attention to kernels which are invariant under rotations and translations. This assumption is satisfied in most important examples.
- We consider positive definite kernels of the form

$$K\colon \mathbb{R}^d \times \mathbb{R}^d \to \mathbb{R}^{d\times d}, \qquad (q_i, q_j) \mapsto k(\|q_i - q_j\|_{\mathbb{R}^d}) I_d$$

where $k\colon (0,\infty) \to \mathbb{R}$ is a scalar function.

Examples:

$$\begin{aligned} k_{1/2}(r) &= \mathrm{e}^{-r} \\ k_{3/2}(r) &= 2(1+r)\mathrm{e}^{-r} \\ k_G(r) &= \mathrm{e}^{-r^2} \end{aligned}$$

Large Deformation Diffeomorphisms Landmark Matching

- We restrict our attention to kernels which are invariant under rotations and translations. This assumption is satisfied in most important examples.
- We consider positive definite kernels of the form

$$K\colon \mathbb{R}^d \times \mathbb{R}^d \to \mathbb{R}^{d\times d}, \qquad (q_i, q_j) \mapsto k(\|q_i - q_j\|_{\mathbb{R}^d}) I_d$$

  where $k\colon (0,\infty) \to \mathbb{R}$ is a scalar function.

Examples:

$$\begin{aligned}
k_{1/2}(r) &= \mathrm{e}^{-r} && = 1 - r + o(r)\ , \\
k_{3/2}(r) &= 2(1+r)\mathrm{e}^{-r} && = 2 - r^2 + o(r^2)\ , \\
k_G(r) &= \mathrm{e}^{-r^2} && = 1 - r^2 + o(r^3)\ .
\end{aligned}$$

Brownian motion of two landmarks

Brownian motion of two landmarks

- The key observation is that for a radial kernel, the distance between the two landmarks is a diffusion process, whose dynamics is characterised by a scalar stochastic differential equation.

Brownian motion of two landmarks

- The key observation is that for a radial kernel, the distance between the two landmarks is a diffusion process, whose dynamics is characterised by a scalar stochastic differential equation.
- $Q = \{q = (x, y) : x, y \in \mathbb{R}^d$ with $x \neq y\}$ and $\lambda = k(0)$.

Brownian motion of two landmarks

- The key observation is that for a radial kernel, the distance between the two landmarks is a diffusion process, whose dynamics is characterised by a scalar stochastic differential equation.
- $Q = \{q = (x, y) : x, y \in \mathbb{R}^d \text{ with } x \neq y\}$ and $\lambda = k(0)$.
- For $q = (x, y) \in Q$,

$$K(q) = \begin{pmatrix} \lambda I_d & k(\|x-y\|_{\mathbb{R}^d}) I_d \\ k(\|x-y\|_{\mathbb{R}^d}) I_d & \lambda I_d \end{pmatrix}.$$

Brownian motion of two landmarks

- The key observation is that for a radial kernel, the distance between the two landmarks is a diffusion process, whose dynamics is characterised by a scalar stochastic differential equation.
- $Q = \{q = (x, y) : x, y \in \mathbb{R}^d \text{ with } x \neq y\}$ and $\lambda = k(0)$.
- For $q = (x, y) \in Q$,

$$K(q) = \begin{pmatrix} \lambda I_d & k(\|x-y\|_{\mathbb{R}^d}) I_d \\ k(\|x-y\|_{\mathbb{R}^d}) I_d & \lambda I_d \end{pmatrix}.$$

- The distance process $(r_t)_{t\in[0,\zeta)}$ between the two landmarks solves the Itô stochastic differential equation

$$\mathrm{d}r_t = \sigma(r_t)\,\mathrm{d}B_t + b(r_t)\,\mathrm{d}t$$

where $\sigma(r) = \sqrt{2(\lambda - k(r))}$ and

$$b(r) = \frac{((d-1)k(r) - \lambda)k'(r)}{\lambda + k(r)}.$$

Brownian motion of two landmarks

Theorem (H, Harms, Sommer – BLMS, 2024)

Let Q be the landmark manifold of pairs of distinct points in $\mathbb{R}^d$. Suppose that k extends continuously differentiable on $(0,\infty)$, and has a bounded and Lipschitz continuous derivative on $[1,\infty)$ such that it defines a positive radial kernel $K\colon \mathbb{R}^d \times \mathbb{R}^d \to \mathbb{R}^{d\times d}$. Moreover, suppose that, for $D,\gamma > 0$, as $r \downarrow 0$,

$$k(0) - k(r) = Dr^{\gamma} + o(r^{\gamma}) \, .$$

Then the Riemannian manifold is Brownian complete if $\gamma \geq 2$, whilst it is Brownian incomplete if $\gamma < 2$.

Brownian motion of two landmarks

Theorem (H, Harms, Sommer – BLMS, 2024)

Let Q be the landmark manifold of pairs of distinct points in $\mathbb{R}^d$. Suppose that k extends continuously differentiable on $(0, \infty)$, and has a bounded and Lipschitz continuous derivative on $[1, \infty)$ such that it defines a positive radial kernel $K \colon \mathbb{R}^d \times \mathbb{R}^d \to \mathbb{R}^{d \times d}$. Moreover, suppose that, for $D, \gamma > 0$, as $r \downarrow 0$,

$$k(0) - k(r) = Dr^\gamma + o(r^\gamma) \ .$$

Then the Riemannian manifold is Brownian complete if $\gamma \geq 2$, whilst it is Brownian incomplete if $\gamma < 2$.

Sketch of proof.

Follow the classification for singular points of one-dimensional diffusion processes by Cherny and Engelbert. $\square$

Numerical simulations

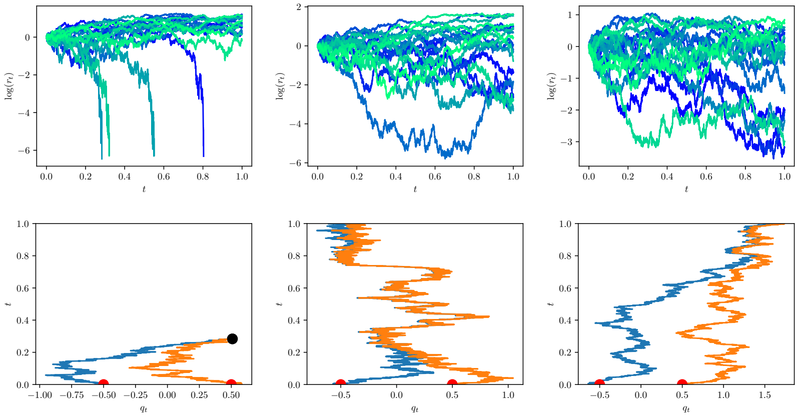

Results for $d = 1$ and $n = 2$ with 20 sample paths. First column for $k_{1/2}$, second column for $k_{3/2}$, and third column for Gaussian kernel. First row shows the log-distances between the landmarks for all sample paths as a function of t, stopped if collision occurs. Second row shows position of the two landmarks versus time for the sample path attaining the smallest inter-landmark distance, again stopped if the landmarks collide.

Numerical simulations

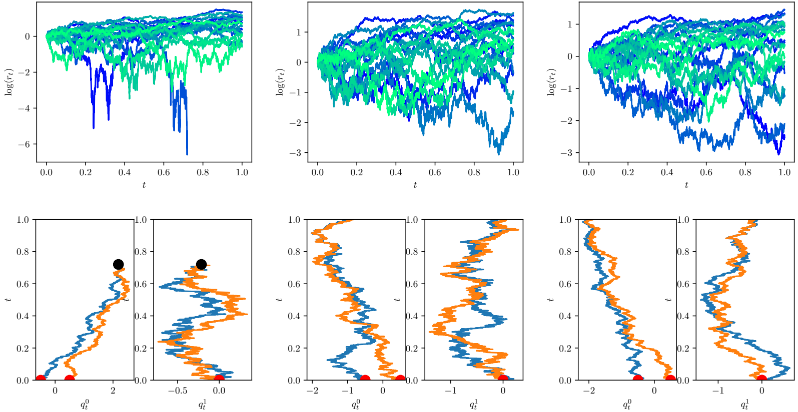

Results for $d = 2$ and $n = 2$. Setup as in the previous figure. In the bottom row, the plots show each coordinate q_t^i, $i = 1, 2$, of the landmarks separately. Whilst the landmarks temporarily come close for all kernels, a rapid decrease in the distance is observed only for the kernel $k_{1/2}$, which indicates collision.